International Journal on Interactive Design and Manufacturing (IJIDeM) (2026) 20:6423–6439
https://doi.org/10.1007/s12008-026-02600-x

ORIGINAL ARTICLE

A visuo-haptic teleoperation platform for demonstration-based programming of force-sensitive robotic tasks

Mohammad Sadeghi[1,2] · **Julio Cesar Ceron Espejo**[1] · **Thorsten A. Kern**[1,2]

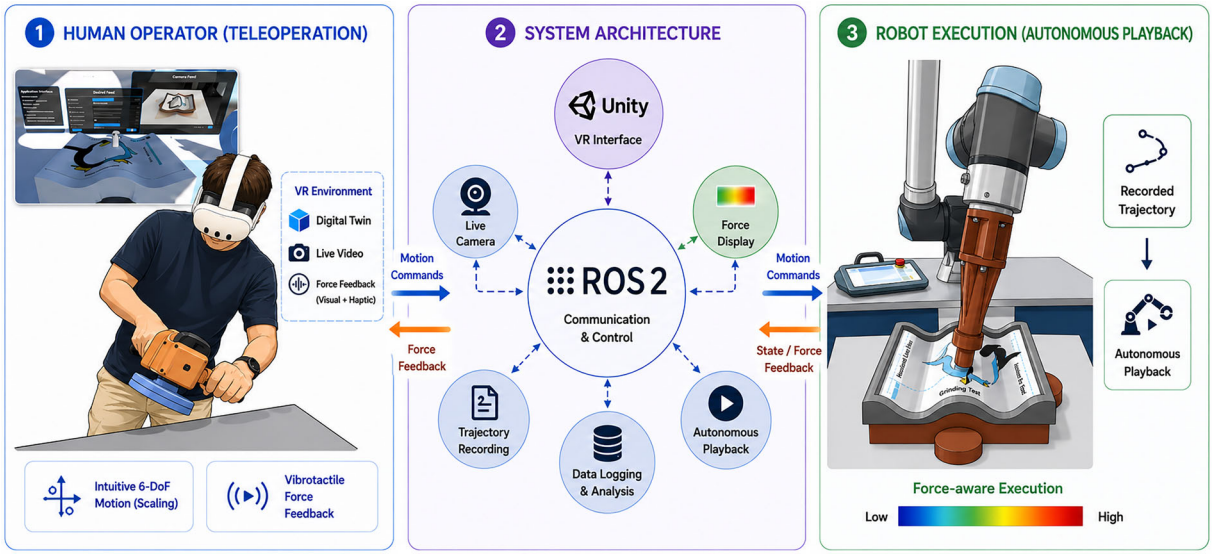
Received: 15 December 2025 / Revised: 13 April 2026 / Accepted: 29 April 2026 / Published online: 19 July 2026
© The Author(s) 2026

Abstract

Industrial processes such as grinding, polishing, and precision assembly demand accurate force regulation and dexterous control. These operations are often repetitive and ergonomically challenging and, in some cases, can pose safety risks to human operators. This paper presents a teleoperation platform for Human–Robot Interaction (HRI) in force-sensitive robotic tasks, incorporating autonomous playback to support intuitive demonstration-based robot programming without complex manual coding. The proposed platform combines virtual reality (VR), optical tracking, and a vibrotactile operator tool within a ROS 2-based control architecture that interfaces with a UR10e industrial robot. A simulated Grinding task was utilized as a proof of concept. The VR environment offers a digital twin of the workspace, live video feedback, and scalable interaction with the workpiece for fine manipulation. Tool odometry generates velocity control commands for intuitive six Degree of Freedom (DoF) motion, while force feedback is conveyed through vibrotactile patterns and a color-coded visual overlay. Experimental validation demonstrated an end-to-end latency below 15 ms and positional errors under 5 mm. Repeatability tests yielded trajectory correlation coefficients (CC) above 0.8. A user study involving 17 participants was conducted to evaluate usability and overall user experience. The results showed high ratings for intuitiveness and system responsiveness, indicating that the proposed platform provides an effective and user-friendly framework for demonstration capture and autonomous replay of force-sensitive robotic operations.

Extended author information available on the last page of the article

Graphical Abstract



Keywords Teleoperation · Robotic · Virtual reality · Demonstration-based programming · Haptic feedback

1 Introduction

Industrial automation has become a foundation of modern manufacturing, driven by the demand for higher productivity, improved product quality, and enhanced workplace safety [1]. Robotic automation in processes such as grinding/polishing [2], and precision assembly [3], remains particularly challenging, as these force-sensitive operations demand not only precise tool positioning but also adaptive force regulation to ensure consistent quality across complex geometries and heterogeneous material properties [4]. Although robots perform repetitive tasks efficiently, they lack the flexibility and precision needed for force-sensitive operations, especially when constant adjustments are required to handle different shapes. These limitations often necessitate human supervision to maintain quality and prevent excessive contact forces, highlighting the importance of intuitive platforms that enable the rapid and reliable transfer of human skills to robotic systems. Beyond these challenges, certain environments such as chemical processing facilities, areas near high temperature furnaces, or aerospace maintenance sites pose significant safety risks or may even be entirely inaccessible to humans, further reinforcing the case for robotic solutions. Traditional robot programming, however, is typically complex, time-consuming, and requires specialized expertise, which constrains scalability and rapid reconfiguration for such applications [5]. To address these challenges, recent advances in Human–Robot Interaction (HRI) and teleoperation technologies have emphasized the integration of Virtual Reality (VR) and haptic feedback to deliver immersive, intuitive control and facilitate the remote operation of robotic systems [6].

The paradigm of Learning from Demonstration (LfD) enables robots to acquire skills through kinematic [7], observation based [8], or teleoperation-based demonstrations [9]. While kinematic demonstrations are suited to simple tasks such as pick and place, teleoperation provides greater versatility, supporting complex operations that demand both positional accuracy and force control. In kinesthetic teaching, Kim et al. [10] showed how material removal rates (MRR) can be generalized to new surfaces using kinesthetic guidance, while Ochoa et al. [11, 12] developed a co-manipulation control architecture for polishing applications. Other studies have investigated direct teaching and replay strategies and force sensor based approaches for surface treatment tasks [13]. Beyond physical demonstrations, virtual interface for polishing skill transfer [14], and a hybrid approach combining kinematic and observation based demonstrations for collaborative leather shoe polishing has been studied [15]. Building on these approaches, immersive environments have further enhanced teleoperation. Virtual Reality (VR) enables naturalistic control and interaction, serving as a medium through which operators can remotely guide robots and generate demonstrations for subsequent learning [16, 17]. Augmented Reality (AR) has also been explored in combination with haptic devices, such as the Phantom Omni [18], to improve immersion. Haptic feedback strengthens task embodiment, while real-time 3D reconstruction and

point-cloud visualization enhance situational awareness [16]. From a control architecture perspective, the Robot Operating System (ROS) framework has become widely adopted for real time teleoperation and surface treatment tasks [11, 19–21]. For example, Ochoa et al. [11] demonstrated polishing with a 7-DOF Sawyer robot using ROS, achieving 50 Hz control for position, orientation, and force data, thereby validating its suitability for near real time applications. ROS has also been integrated with VR to extend teleoperation capabilities [20, 21]. Frameworks such as ROS Reality [19] and mixed-reality (MR)-based systems [20] enable immersive robot control, while middleware tools including ROS# and Rosbridge [22] facilitate real time synchronization with Unity. Latency remains a critical factor in the performance and safety of teleoperated robotic systems [23]. Research indicates that for effective real time control, the total round-trip latency, including sensing, transmission, processing, and actuation, should remain below 100 ms, with target values under 50 ms for high-precision tasks [23, 24].

Despite advances in immersive teleoperation and LfD, many platforms are not designed for demonstration learning and lack dedicated tools for simulating force-sensitive tasks in 3D space. Workspace scaling is often restricted to application level zooming rather than integrated into the control framework. To the best of the authors' knowledge, no comprehensive studies have evaluated industrial robot performance in such platforms with respect to responsiveness, repeatability, and reliability. Current teleoperation frameworks also rarely incorporate force-aware trajectory learning, which is essential for tasks that require precise contact interaction. Although ROS2 provides strong capabilities for real time communication and modular control, its potential remains underutilized in integrated systems that combine VR control, haptic feedback, and autonomous playback. Moreover, active workspace scaling and visuo-haptic feedback tools are absent from prior implementations, leaving a gap for a comprehensive platform tailored to force-sensitive industrial applications.

This study presents an innovative visuo–haptic feedback teleoperation platform designed to facilitate intuitive human–robot interaction and demonstration-based robot programming in force-sensitive robotic tasks. The robot motion is controlled through velocity commands derived from the odometry of a Vive Ultimate Tracker mounted on the operator's tool, enabling intuitive six-degree-of-freedom (6-DOF) control in real time. The platform supports both direct teleoperation and autonomous playback of recorded demonstrations, establishing a flexible demonstration-based programming workflow. A simulated grinding task was employed as a proof of concept, with validation results demonstrating good trajectory repeatability and system responsiveness through workspace scaling. It should be mentioned that the task was designed as a controlled surface interaction experiment to evaluate teleoperation performance and trajectory reproducibility rather than manufacturing process outcomes. Within the virtual environment, a color-coded force indicator provides both numerical and visual feedback, assisting operators in maintaining appropriate contact forces during surface interaction. Furthermore, a user study was conducted to evaluate usability and intuitiveness, confirming the practicality and potential of the proposed system for demonstration-based robotic task programming. The objective of this study is to develop and experimentally evaluate the proposed visuo–haptic teleoperation platform in terms of system latency, trajectory repeatability, force interaction behavior, and user experience. The experimental findings highlight the system's capability to enable reliable demonstration capture and autonomous trajectory replay within acceptable limits of latency and force accuracy.

2 Materials and methods

The methodology is presented in four stages. It begins with the conceptual design, which establishes the engineering requirements for both the operator and robot domains. This is followed by the system architecture and integration, where the hardware and software elements are specified and their coordination within the workflow is described. The teleoperation framework is then introduced, encompassing the ROS2 implementation and the combined virtual reality and haptic interface. Finally, the system evaluation is presented, including the experimental setup and the measurement protocols used for performance assessment.

2.1 System architecture

The platform was conceived based on operator-centered requirements that combined quantitative performance targets with qualitative usability features. Quantitative specifications included an end to end latency below 15 ms, positional accuracy in the range of 1 mm, workspace scaling between 1.0 and 10.0, and haptic forces in the range of 0–23 N. Qualitative aspects emphasized the development of an intuitive VR interface, multimodal visual and haptic feedback, ergonomic tool interaction, and robust safety mechanisms. From the operator's perspective, movements of the handheld tool are captured in six degrees of freedom and translated into velocity commands that drive the robot in real time. The robot's responses are conveyed back to the operator through multiple feedback channels: vibration based haptic cues, color-coded visual overlays, and numerical force indicators. These feedback mechanisms are complemented by a virtual environment that provides a digital twin of the

task surface as well as a live video feed from the robot's workspace.

To meet these requirements, the hardware configuration was designed around the UR10e 6-DOF industrial manipulator as the primary robot. A custom designed tool tip was developed to simulate force interactions on a grinding surface, while both two dimensional and 3D test surfaces were prepared to evaluate system performance under varied geometries. On the operator side, a VR headset delivers the immersive environment, and a custom handheld tool replicates the form of a grinding device. This tool integrates haptic feedback to reproduce perceived force levels for the user, while motion in 3D space is tracked wirelessly through a Vive Ultimate Tracker attached to the operator tool. At the software level, the Tracker is integrated via SteamVR, which functions as the runtime environment responsible for handling its positional and orientation data. Moreover, ROS 2 serves as the middleware for communication between the system components. The ROS-Bridge suite enables JSON-based communication, allowing non-ROS clients to interact with the ROS ecosystem through topic publishing and subscription. In parallel, Unity provides the main VR environment, and together with the ROS–Unity Visualization Package, supports real time visualization of incoming and outgoing messages in the virtual workspace.

The overall system architecture is presented in Fig. 1. On the robot side, the framework operates on a Linux environment hosted within a Docker container, with ROS 2 Jazzy running on Ubuntu 22.04 and MoveIt2 employed for motion planning and control. The robot's tool center point (TCP) is fitted with a marker that interacts with the target surface, while a camera mounted near the robot streams live video of the workspace. On the operator side, a Windows 10 workstation is utilized to meet hardware compatibility requirements. This workstation communicates wirelessly with the custom operator tool, which is based on an ESP32 microcontroller. For stable operation, both the robot and operator computers must remain on the same network to support ROS-based communication and maintain seamless data exchange. Additional details of the finite state machine governing both teleoperation and autonomous modes are provided in Supplementary Figure S1.

2.2 Control strategy

The ROS2 architecture of the proposed system employs a forward position controller in combination with MoveIt Servo to address both teleoperation and autonomous control requirements. MoveIt Servo provides two primary command interfaces, Twist Control and Pose Control. In this study, Twist Control was employed to achieve real time mirroring of operator movements, whereas Pose Control was utilized for predefined positioning tasks. For velocity regulation, the system computes Cartesian velocity commands based on the pose error between the tracked tool pose and the robot's current pose. These commands are transmitted through ROS2 and executed by MoveIt Servo, while the UR10e internal controller performs the low-level joint servo control. This approach generates Cartesian velocity commands by calculating the pose error between the tracked tool pose and the robot's current pose, both expressed in a common coordinate frame. The position error e_p is determined according to Eq. (1), and serves as the basis for computing the velocity input to the robot controller.

$$e_p = \frac{\overrightarrow{p}_{tracker}}{s} - \overrightarrow{p}_{robot} \tag{1}$$

The scale factor s

$$p_{next} = \overrightarrow{p}_{tracker} + v_{lin}.\Delta t \tag{3}$$

To prevent singularities or self-collisions, velocity commands were constrained by setting them to zero whenever a component attempted to drive the robot beyond its workspace limits. This safety layer was implemented using a culling function in ROS. The logic of the control nodes is illustrated in Fig. 2.

The proposed system follows a command-based teleoperation architecture in which the operator's motion is translated into Cartesian velocity commands that are transmitted to the robot through ROS2 and executed via MoveIt Servo. The UR10e industrial robot performs the low-level joint servo control internally through its built-in controller, which ensures stable trajectory tracking within the robot's operational limits. Consequently, the teleoperation interface does not implement a new control law but rather provides high-level velocity references to the industrial robot controller. It should be noted that the platform does not employ bilateral force-reflecting teleoperation. Interaction forces measured at the robot are used only to generate vibrotactile and visual feedback cues for the operator and are not fed back into the robot control loop. Therefore, the system does not form a closed human–robot–environment force-control loop. The stability of robot motion is thus governed primarily by the internal robot controller and the bounded velocity commands generated by the teleoperation interface.

2.3 Teleoperation framework

This section presents the communication framework developed for the teleoperation system, outlining the structure and interaction of its ROS2 nodes and topics. An overview of the application workflow is also provided, describing how the teleoperation mode enables real time robot control and operator data recording.

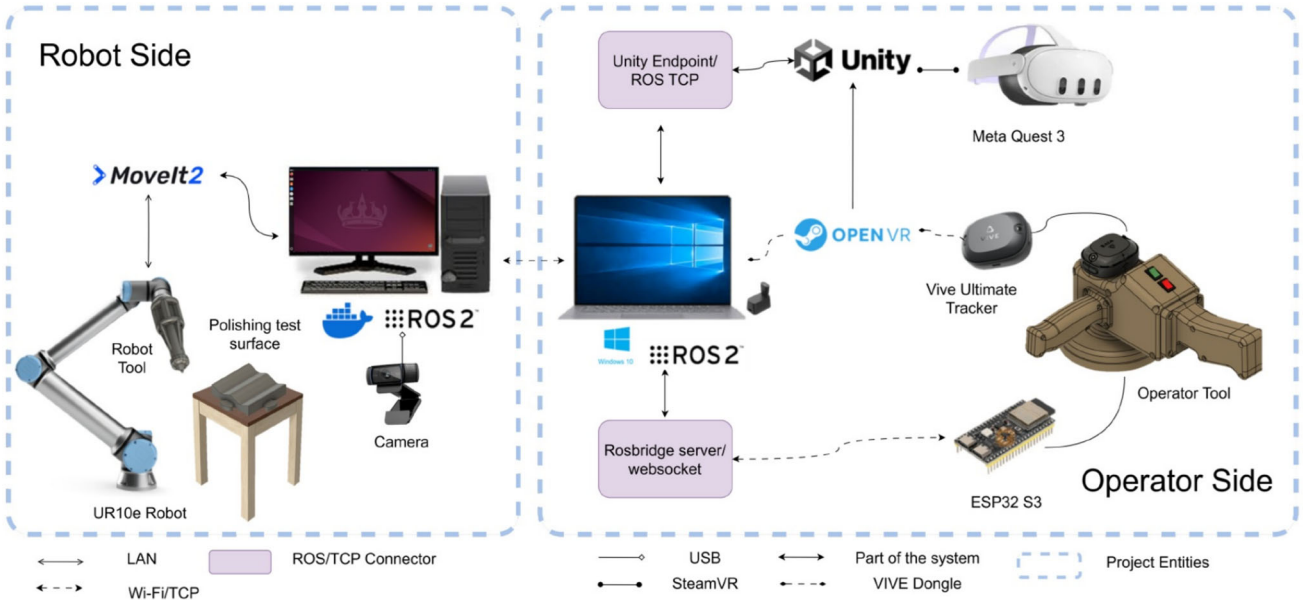


Fig. 1 Overview of the proposed system architecture, illustrating the main components and supporting technologies

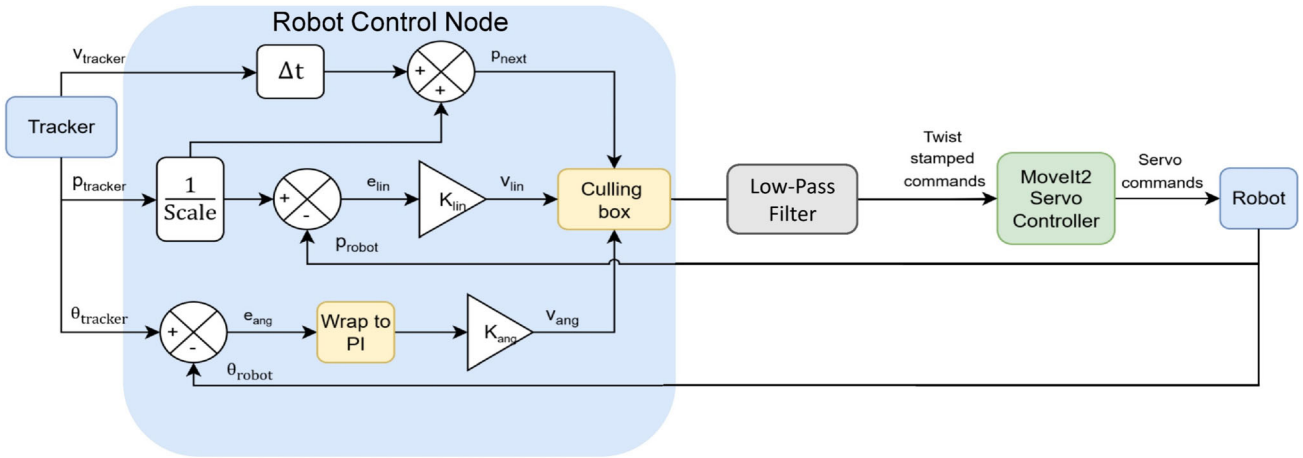


Fig. 2 Velocity control node architecture

2.3.1 Implementation of robot communication

The teleoperation framework was developed using a modular ROS 2 architecture, as illustrated in Fig. 3. It is structured around four principal nodes: the Robot Node on the robot side and three nodes on the operator side including Tracker Node, Tool Node, and Unity Node. Each node exchanges information through a series of dedicated ROS 2 topics that support both teleoperation and autonomous operation modes. The Operator Tool Node manages interaction with the physical handheld device and the tracking system. It handles calibration procedures, establishes a zero-reference frame, and interprets button commands to initiate robot motion, record trajectories, or trigger safety actions such as emergency stop. Tool status messages are published via $/tool_status_topic$. Together, these nodes and communication topics establish an integrated data exchange pipeline that synchronizes sensing, and robot control, enabling precise teleoperation and reliable autonomous execution.

2.3.2 Virtual reality interface

The Unity software (Unity-engine, Version 6) was used to develop the VR interface. The virtual workspace replicates the robot setup, consisting of a marker-equipped UR10e manipulator, a camera, and a configurable test surface for simulated grinding tasks. The overall view of the application is shown in Fig. 4a–d. The interface layout is divided into three interactive panels. The status panel displays the live operational state of the robot, tracker, and operator tool,

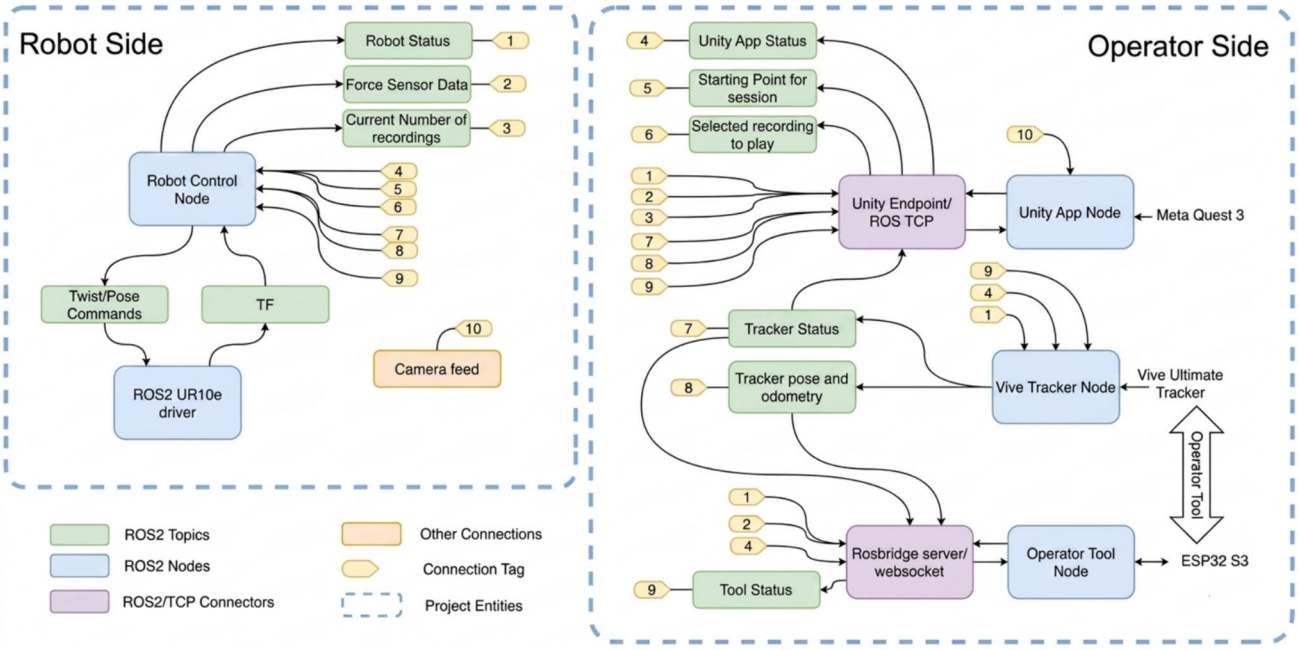


Fig. 3 ROS 2 node and topic architecture of the teleoperation framework, showing communication flow between the robot side and operator side

together with real-time velocity and force data to verify node connectivity. As shown in Fig. 4a, the interaction panel allows the user to select operational modes and adjust parameters. In the virtual scene, the operator tool is visually represented with handles, buttons, and a color-coded pen tip that changes hue according to the applied contact force, as depicted in Figs. 4b–c. The color scale is defined as white (no contact), green (1–10 N), yellow (11–20 N), and red (21–23 N). A miniature camera feed and force indicator are also displayed on the tool to enhance situational awareness. Two primary modes of operation are supported. In teleoperation mode, the system synchronizes the real and virtual tools after a calibration step, allowing the operator to perform grinding tasks with real time visual and haptic feedback. The tool path is visualized through dynamically generated meshes and particle effects, while robot motion and interaction forces are recorded for subsequent playback. The particle effect enhances immersion by visually simulating material removal from the surface during the grinding process, as illustrated in Fig. 4b. The scaling mechanism aligns the VR environment with the physical robot workspace by computing a new initial robot position based on the scaling factor s and the tool's coordinates in Unity. A fixed vertical distance of 21 cm is preserved between the guide position marker and the highest point of the surface by means of the offset term h_{off}, as defined in Eqs. 4–6.

$$x_r = x_0 + \frac{(z_g - z_{ref})}{s} \tag{4}$$

$$y_r = y_0 + \frac{(x_g - x_{ref})}{s} \tag{5}$$

$$z_r = z_0 - h_{off} + \frac{h_{off}}{s} \tag{6}$$

Here, x_r, y_r, and z_r denote the robot's starting coordinates, while x_0, y_0, and z_0 correspond to its home position at a unit scale ($s = 1.0$). The variables x_g and z_g represent the tool coordinates in the VR environment, referenced against the fixed object (x_{ref}, $and z_{ref}$). This formulation ensures that operator movements in Unity are proportionally mapped to the robot workspace while preserving a constant vertical reference.

In autonomous mode, the robot executes previously recorded trajectories selected through the VR interface. The operator can initiate, pause, or stop playback, while the system monitors force thresholds to ensure safe execution. This mode enables reliable reproduction of human-demonstrated motions without requiring continuous operator input. More details on the data flow of the teleoperation and autonomous mode are provided in Supplementary Figure S2 and S3. Moreover, a short video demonstrating both the application and the robotic platform is provided in Supplementary Clip S1 for better illustration of the process.

2.4 Experimental setup and characterization

Figure 5a-b illustrates the experimental apparatus, including both hardware and software components. To assess

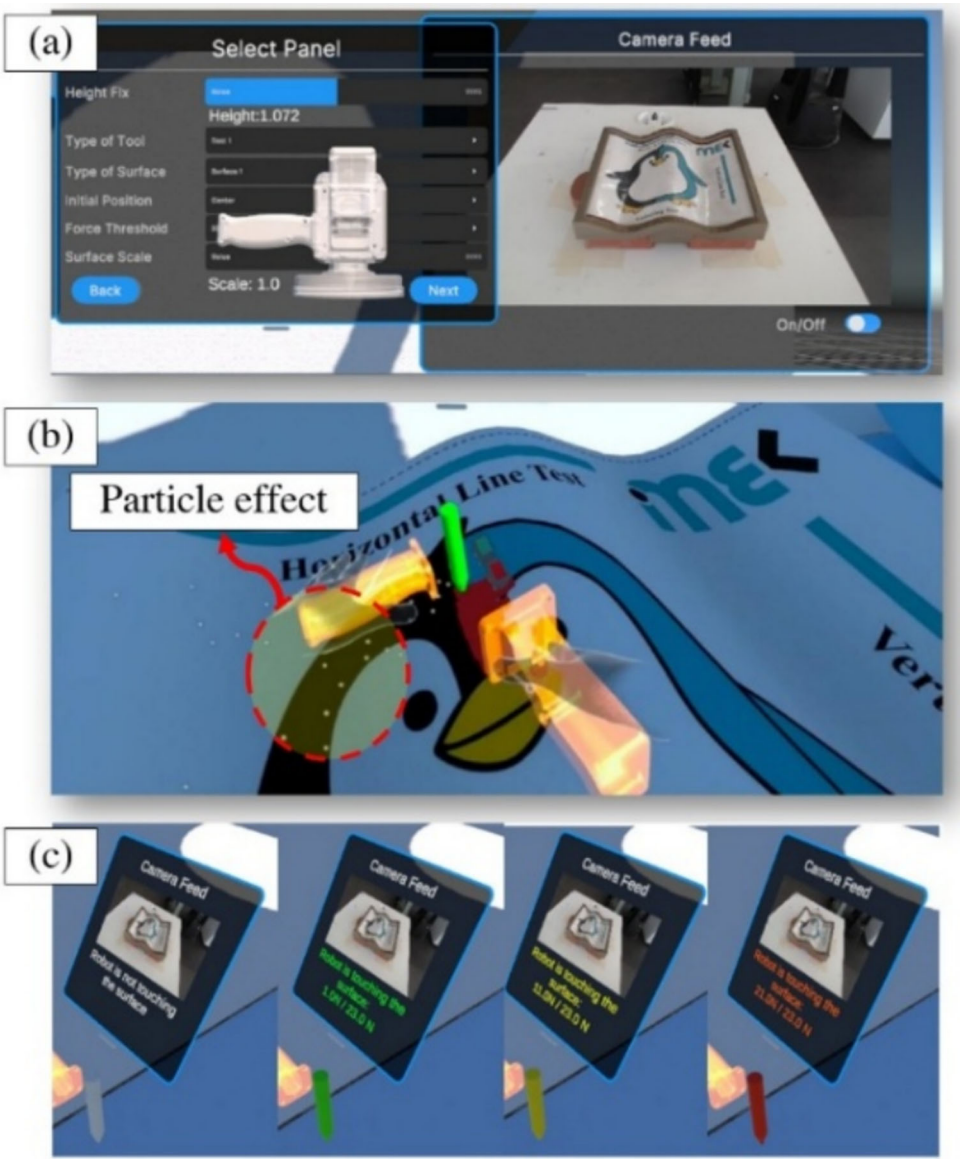


Fig. 4 Virtual Reality (VR) interface; (**a**) status and interaction panels with parameter selection and camera feed, (**b**) particle effects simulating material removal, and (**c**) color-coded force feedback for operator force awareness

the responsiveness and positional accuracy of the UR10e collaborative manipulator (Universal Robots A/S, Odense, Denmark) in a simulated grinding task, the tool center point (TCP) was equipped with a marker holder (Fig. 5b1), enabling the robot to perform writing tasks on a custom designed test surface (Fig. 5b2). A camera was installed to monitor the workspace, thereby complementing the virtual reality (VR) interface with an additional visual feedback channel.

A custom handheld operator tool was designed and manufactured via 3D printing (Bambu Lab X1, Shenzhen, China) to replicate the ergonomics of a grinding instrument (Fig. 5a1). A VIVE Ultimate Tracker (HTC Corporation, Taiwan) was mounted on the device to record the operator's hand kinematics. The tracker employed inside out tracking using embedded cameras and onboard computation, eliminating the need for external base stations. Wireless communication was established through a 2.4 GHz protocol, transmitting 6-DOF pose and velocity data at 500 Hz. This high update rate enabled real time and stable mapping of operator movements to robot commands.

To render haptic cues, four eccentric rotating mass (ERM) actuators were embedded along each side of the tool handle, as depicted in the inset of Fig. 5a1. These actuators generated directional vibration feedback proportional to the force measured at the robot's end effector. When the tool moved in a given direction, the corresponding actuators were sequentially triggered, eliciting a perception of directional motion for the operator. Force regulation during the experiments was informed by established guidelines indicating that maintaining contact forces between 17 and 22 N is optimal for high quality surface finishing. Real time force measurement was

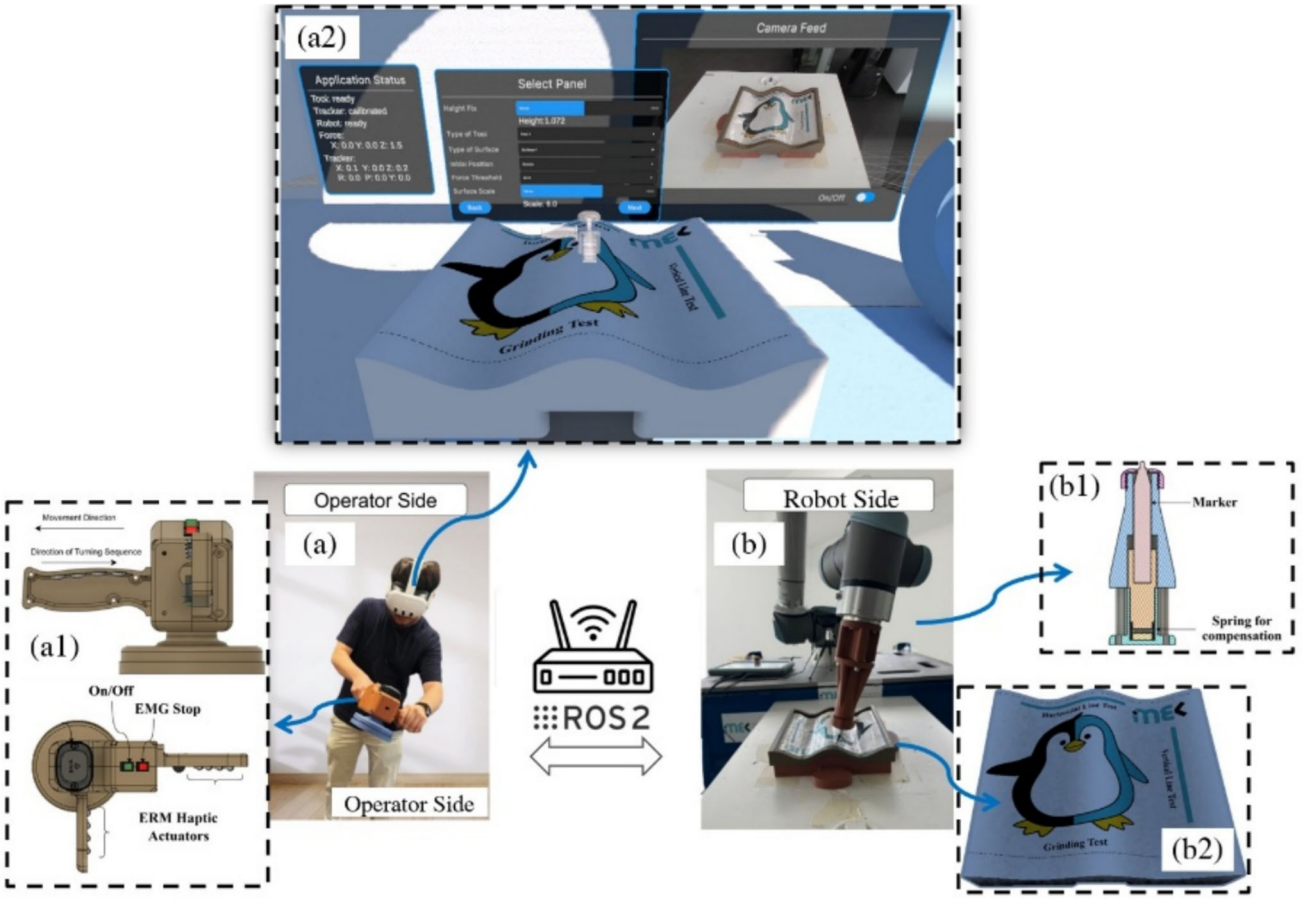


Fig. 5 Measurement apparatus. (**a**) Operator side, including; (**a1**) inset of the handheld tool design; and (**a2**) inset of the VR application layout; (**b**) Robot side, including (**b1**) inset of the marker holder design and (**b2**) inset of the simulated test surface

achieved using the internal force/torque sensor of the UR10e, which provided a resolution of 0.1 N and an accuracy of up to 2% of the full scale range (300 N). This corresponded to a maximum measurement error of approximately 6 N, ensuring reliable force acquisition throughout the trials. An extension with additional force sensing at the TCP could be readily implemented to further reduce contact forces; however, it was not identified as necessary in the test scenarios. The VR environment was implemented on a Meta Quest 3 headset (Meta Platforms, Inc., USA), operating at a native refresh rate of 90 Hz (Fig. 5a2).

The tracker's spatial resolution was validated using a 3D spiral motion test in which it was rigidly mounted on the robot's TCP, ensuring that both the tracker and the robot followed the same physical trajectory. The data were then compared to the internal sensor of the UR10e robot as a reference. The results validated an acceptable average deviation of 1.7 mm, 1.2 mm, and 0.9 mm for the X, Y, and Z directions, respectively, as illustrated in Fig. 6. It should be noted that, in order to achieve higher accuracy, a low-pass filter was implemented to reduce deviation errors, as depicted in Fig. 2.

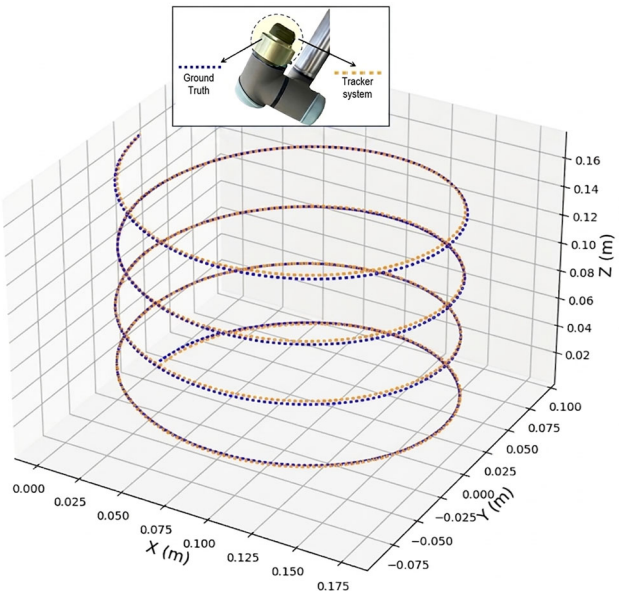


Fig. 6 Validation of the tracker's position accuracy relative to the UR10e's internal sensor across all axes

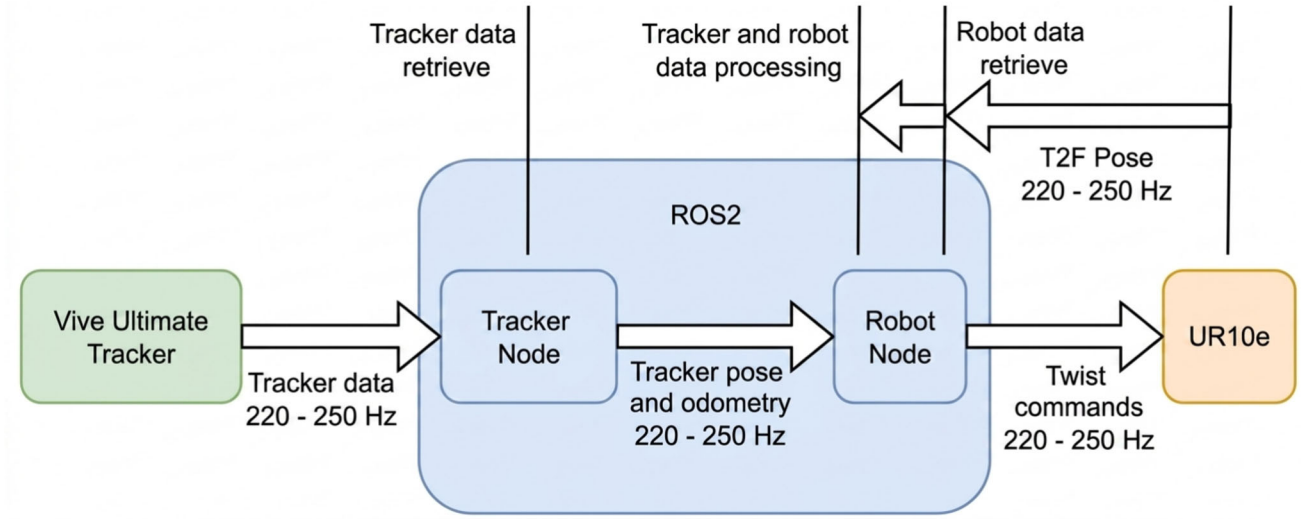


Fig. 7 Communication latency from the tracker to the robot for achieving velocity control

In terms of temporal resolution, the control loop of the system was designed to operate at 500 Hz, meaning each stage should ideally process data within 2 ms. However, due to hardware and communication constraints, the effective update rates observed in ROS varied between 220 and 250 Hz, resulting in actual cycle times of approximately 4–4.5 ms. Figure 7 depicts the data path from the VIVE Ultimate tracker to the robot motion, which consisted of several steps. High frequency topics, such as tracker pose and odometry (ideally updated at 500 Hz), could not be processed reliably within Unity. To address this, an independent Python-based ROS 2 node using the OpenVR API was implemented to manage high rate, low latency tracker data publishing. Conversely, lower frequency topics, such as Unity status updates (e.g., application state and user actions), were transmitted at 10 Hz, which was sufficient for system requirements.

2.5 Measurement scheme

The proposed teleoperation platform was evaluated through a structured measurement scheme addressing both technical performance and user interaction. A simulated grinding task was implemented, where the robot, equipped with a marker at the TCP, executed vertical and horizontal lines as well as a penguin coloring task on flat and wavy test surfaces as shown in inset of Fig. 5b2. These trials were conducted at workspace scaling factors of 2 × and 6 × to examine pose error, force regulation, and adaptability to task complexity. Force data were obtained from the UR10e's internal force/torque sensor and benchmarked against recommended thresholds for grinding operations. To assess usability and repeatability, a user study was carried out with 17 participants. Each participant performed the three tasks at both scaling factors, and task outputs were analyzed through image processing. Participant drawings were aligned with template images using a homography transformation estimated via the RANSAC algorithm, which robustly fits geometric correspondences while rejecting outliers. From the aligned images, binary masks were generated to compute coverage (percentage of target area correctly filled) and overdraw (percentage of ink placed in non-target regions). A performance score was then derived from the difference between coverage percentage and overdraw percentage. Additional evaluation metrics included trajectory accuracy, repeatability, and Correlation Coefficients (CC). The correlation coefficient was computed to evaluate the similarity between trajectories executed by the operator and those reproduced autonomously by the robot. This analysis quantified the degree of alignment between the human-performed path and the corresponding playback trajectory recorded by the system. By comparing the positional data of both trajectories, the CC value served as an indicator of how effectively the teleoperation platform transferred the operator's motion skills to the robot during autonomous execution. Finally, participants completed a post experiment questionnaire to capture subjective evaluations of intuitiveness, responsiveness, and ergonomics. More details about image processing and correlation analysis can be found in the supplementary file, Sections S3.1 and S3.2, respectively.

3 Results and discussion

Besides the objective measurements, the key performance metrics are linked to an objective evaluation in scenarios near to a realistic application. In the following, a quantitative task-performance analysis and a force- and position-accuracy

Table 1 Performance scores for flat and wavy test surfaces at a scaling factor of 6

	Surface type	Performance (%)
2d Flat	Vertical line	75.77
	Horizontal line	47.30
	Penguin shape	74.90
3d Wavy	Vertical line	71.20
	Horizontal line	73.20
	Penguin shape	67.31

analysis of human test subjects are presented, extended by a repeatability test of trained trajectories.

3.1 Performance analysis

This section focuses on a quantitative evaluation of participants' ability to accurately fill the assigned target areas during the experimental tasks. Representative samples of the image data used for this assessment are presented in Fig. 8a-d. The Fig. 8a-b illustrates the unprocessed outcomes of the user performed on both flat and wavy surfaces, whereas the Fig. 8c-d shows the corresponding outputs after applying the image processing algorithm. The resulting color overlays provide a visual summary of task performance: green indicates correctly covered regions, red highlights areas of overdraw, and blue marks sections where under-coverage occurred.

Table 1 summarizes the computed performance scores across the different task and surface conditions. The highest score was obtained for the vertical line task on the flat surface (75.8%), followed closely by the penguin coloring task on the same surface (74.9%). Although the penguin task on the wavy surface exhibited high coverage, its overall score decreased to 67.3% due to a higher level of overdraw. For the horizontal line task, performance on the wavy surface (73.2%) exceeded that on the flat surface (47.3%). In general, the vertical and penguin tasks conducted on flat surfaces produced the most consistent and accurate results, while the horizontal task on the flat surface demonstrated the lowest performance. Despite achieving relatively high coverage, tasks on wavy surfaces showed a decline in overall score as a result of increased overdraw, highlighting the greater challenge of maintaining precise motion over non-uniform geometries. The lower performance observed in horizontal tasks compared to vertical ones can be attributed to a combination of ergonomic and scale-dependent factors. During horizontal movements, the operator's wrist and forearm adopt less stable postures, increasing motion variability and reducing fine motor precision. This effect becomes more pronounced at higher workspace scaling factors, where the operator must cover a wider range of motion to complete the task. In vertical trajectories, users can more naturally adjust their body position or step along the path to maintain alignment with the desired trajectory. In contrast, horizontal paths are often compensated for primarily through wrist and arm movements, leading to less consistent coverage and greater overdraw. These differences also depend on individual user skill and comfort with the teleoperation interface. To verify that the system performance and robot motion accuracy were consistent along both testing scenarios, a position accuracy test was conducted, as presented in the following section. It should be emphasized that the initial comparison between the flat and 3D wavy surfaces was conducted with a single participant. Thereafter, a user study with multiple participants was carried out using only the flat surface to validate the findings, as detailed in Sect. 3.4.

3.2 Position accuracy and force analysis

Regarding user motion during the penguin coloring task, Fig. 9a-b show the trajectories followed on the flat and wavy surfaces, respectively. On the wavy surface, users frequently lifted the tool to reposition it for more precise coloring. To improve visualization, data points corresponding to moments when the tool was not in contact with the surface were removed from the dataset. Analysis of the recorded data revealed that the mean position error along the X-axis was 1.1 mm on the flat surface and 0.7 mm on the wavy surface, with similarly small deviations observed in the Y and Z directions. Orientation errors also remained minimal, consistently below 0.01 radians for roll, pitch, and yaw. These findings demonstrate that tracking accuracy was preserved with negligible variation when transitioning from flat to wavy geometries. Figure 9c-d illustrate the recorded trajectories of the robot, color-coded according to the magnitude of the contact force during the penguin coloring task. On both surfaces, the applied forces remain within the desired operational range, demonstrating effective control of contact interaction. The flat surface exhibits a more uniform force distribution, indicating stable tool contact and consistent pressure throughout the motion. In contrast, the wavy surface shows greater variation in force magnitude, particularly at regions of curvature.

Table 2 provides a detailed quantitative comparison of the measured force levels across all task conditions. As observed, the mean forces for the vertical and horizontal line tasks were nearly identical between the flat and wavy surfaces. For the vertical line, the average forces were 1.67 N on the flat surface and 1.64 N on the wavy surface, whereas the horizontal line task yielded 2.96 N and 2.80 N, respectively. The largest discrepancy was found in the penguin coloring task, where the wavy surface required a higher mean force and a considerably greater peak force (11.68 N versus 7.77 N). This

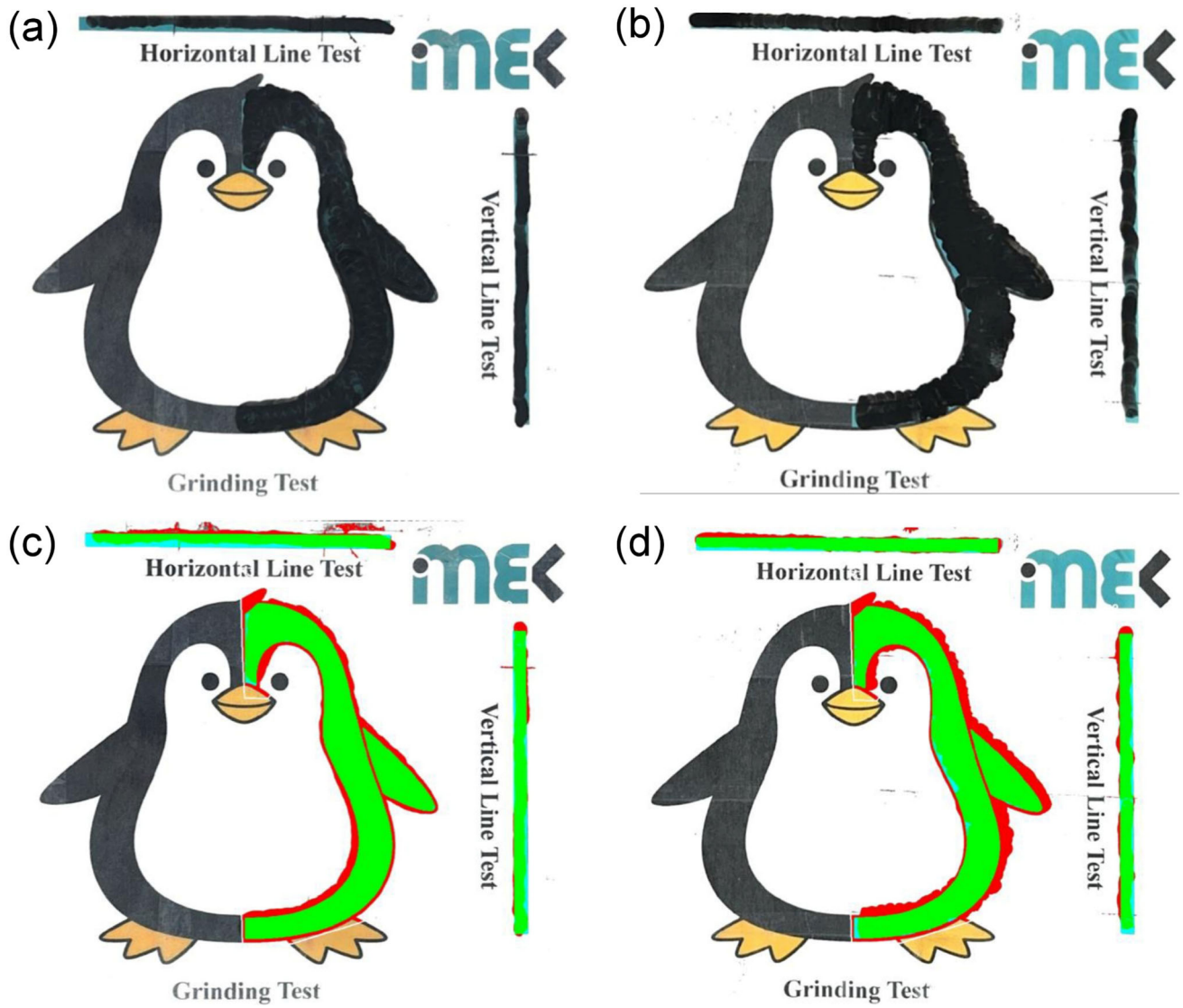


Fig. 8 Performance assessment of the simulated grinding task on flat and wavy surfaces. (**a**) Original flat surface and (**b**) original wavy surface; (**c**) processed image of the flat surface and (**d**) processed image of the wavy surface. For better visualization, the wavy 3D surface was mapped onto a 2D plane

increase can be attributed to the additional effort needed to sustain uniform contact and correct tool orientation over the uneven surface geometry, along with potential minor calibration offsets in the tracking system. Despite these fluctuations, force levels remain well below the safety threshold, confirming the system's ability to adapt to uneven geometries without excessive force application.

3.3 Repeatability test

Figure 10 illustrates the repeatability outcomes for all task types performed on both flat and wavy surfaces, represented through correlation coefficients. The results indicate high consistency across tasks, with the penguin coloring task on the flat surface achieving the highest correlation value (0.95). Lower repeatability was observed on the wavy surface, where the vertical and horizontal line tasks yielded correlation coefficients of 0.84–0.79, respectively. The decline in repeatability on the wavy surface may be attributed to systematic errors, potentially influenced by network bandwidth constraints that affect the transmission rate of positional data points.

In addition, the observed differences between task types can be explained by the interaction between human motor control, visual feedback, and trajectory characteristics in the teleoperation setup. The horizontal line represents a highly constrained motion requiring continuous precision along a single axis, where small deviations directly accumulate into

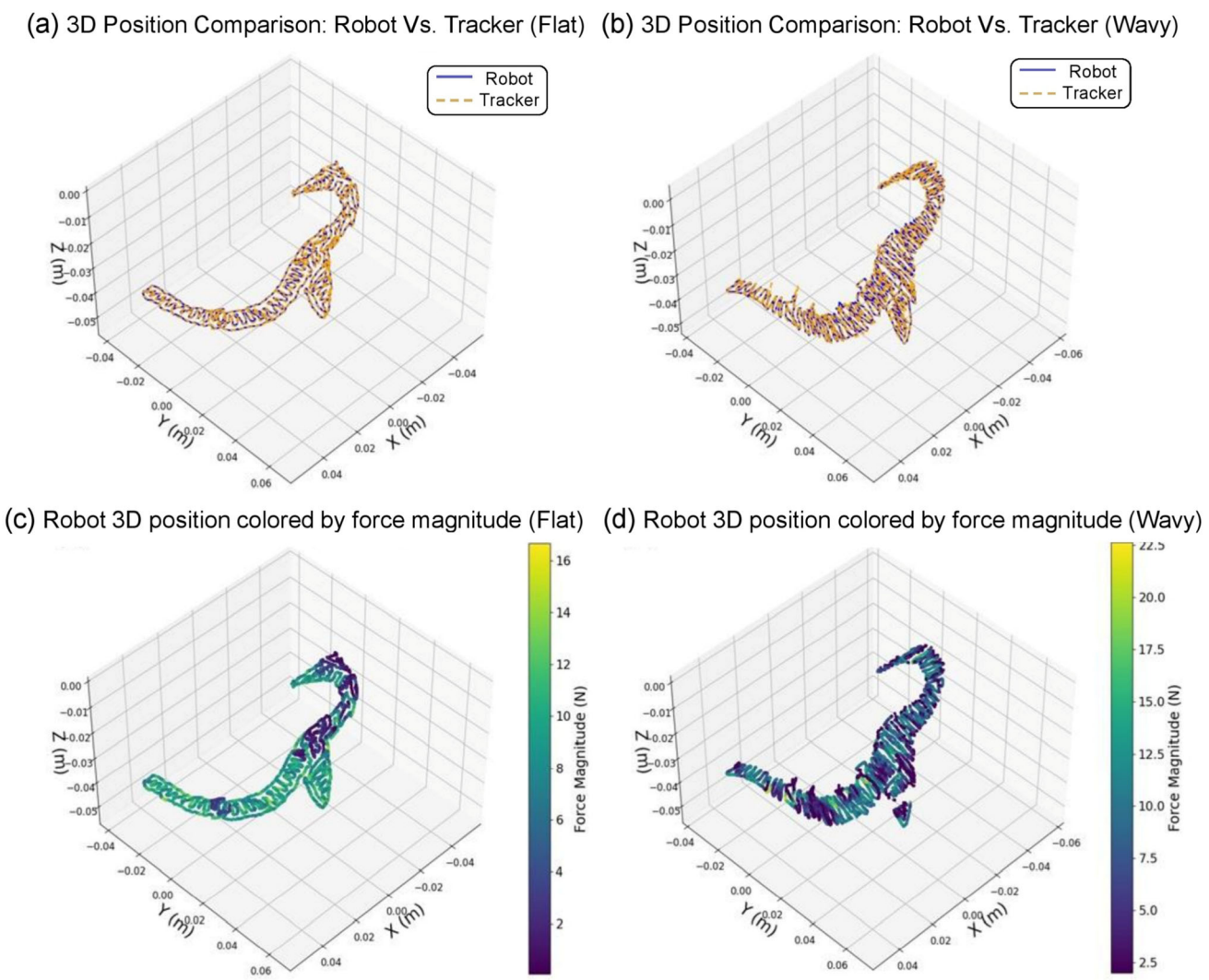


Fig. 9 Evaluation of position accuracy and applied force magnitudes during the simulated grinding task of a penguin shape on different surfaces: (**a**) trajectory on a flat surface, and (**b**) wavy surface, (**c**) force magnitude on a flat surface, and (**d**) wavy surface

Table 2 Experimental evaluation of contact forces on flat and wavy surfaces

Type/Level [N]	Vertical line			Horizontal line			Penguin		
	Min	Mean	Max	Min	Mean	Max	Min	Mean	Max
Flat	0.04	1.67	6.34	0.11	2.96	7.09	0.02	3.44	7.77
Wavy	0.01	1.64	8.89	0.02	2.80	8.85	0.67	3.69	11.68

noticeable errors. In contrast, vertical motion benefits from more stable shoulder–elbow coordination and alignment with the user's body frame, enabling improved trajectory control and reduced drift. Furthermore, under increased motion scaling (scale = 6), horizontal movements occasionally required users to physically reposition or take small steps to maintain a comfortable interaction workspace, introducing additional instability and contributing to higher tracking errors. The penguin-shaped trajectory, despite its geometric complexity, provides rich visual features such as curves and edges that allow users to perform continuous micro-corrections during motion, thereby reducing error accumulation compared to simple linear trajectories. Finally, motion scaling amplifies small hand movements in the robot workspace, disproportionately affecting straight-line tasks while having a reduced impact on complex trajectories with varying curvature.

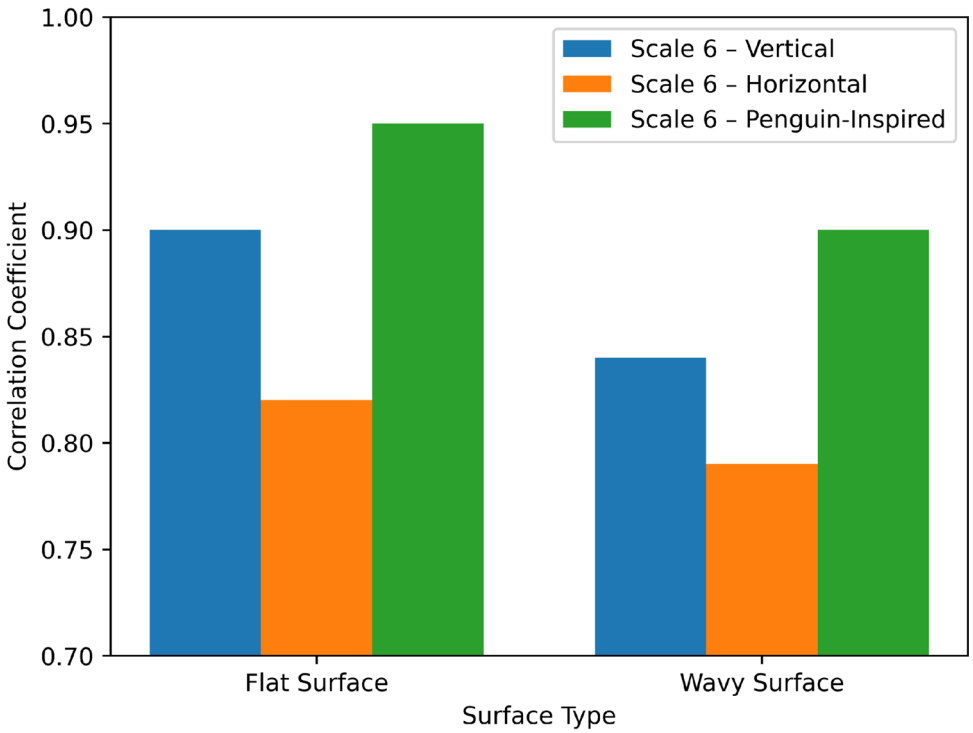


Fig. 10 Comparison of user-performed and autonomous robot trajectories, with correlation coefficients for the flat and wavy surfaces, used to assess skill transfer effectiveness

3.4 User experience test

User experiments with 17 participants were conducted on the 2D surface to assess the usability and overall user experience of the proposed skill-transfer platform, following prior validation of the system's performance on both 3D and 2D surfaces. To evaluate the relationship between task accuracy and completeness, a performance value was calculated for each participant by subtracting the overdraw percentage from the coverage percentage. The resulting score distributions are depicted in Fig. 11. In the visualization, cooler tones correspond to better performance, characterized by extensive coverage and minimal overdraw, whereas warmer tones denote less efficient task execution. The heatmap highlights consistently strong outcomes in the scale 6 Penguin and scale 6 vertical straight-line tasks, with several instances exceeding 70%. The average scores recorded for each condition were 47.08% for the scale 2 Vertical task, 57.07% for the scale 6 Vertical task, and 70.10% for the scale 6 penguin task. Among these, the penguin task exhibited not only the highest mean score but also the lowest dispersion, reflecting uniform user performance. For the vertical trajectory, scale 6 produced values roughly 15 percentage points higher than scale 2, demonstrating the advantage of an expanded workspace that minimizes overdraw and enhances coverage. The variability assessment further supports that larger-scale configurations lead to greater consistency, while smaller scales intensify the effects of minor alignment deviations.

To evaluate trajectory consistency among participants, correlation coefficients were calculated for experimental tasks conducted at Scale 6. As presented in Table 3, all tasks achieved mean correlation values above 0.85, indicating strong repeatability across trials. The highest correlation was obtained in the Scale 6 Penguin task, demonstrating the robustness and stability of the proposed system. It should be mentioned that a slight systematic deviation was detected, which may be attributed to tracker calibration inaccuracies and limitations in data transmission rate. Such fluctuations can influence motion precision, as robot accuracy depends directly on the velocity commands transmitted. Additional investigation is required to further improve the communication and calibration procedures. Further details on the correlation coefficient analysis for participants are provided in Supplementary Figure S4.

To gain insights into participants' user experience, a post-experiment questionnaire was designed and administered after they interacted with the proposed human–robot skill transfer platform. The questionnaire evaluated several parameters, including ease of understanding, comfort, intuitiveness, immersiveness, haptic feedback, and the effectiveness of the scaling feature on performance. Figure 12a–c presents participants' evaluations of the system's immersiveness, haptic feedback, and scaling functionality. As shown in Fig. 12a, 65% of participants rated the virtual environment as very immersive, while 23% described it as immersive. These outcomes suggest that most users experienced a high level of engagement with the VR interface, an important factor

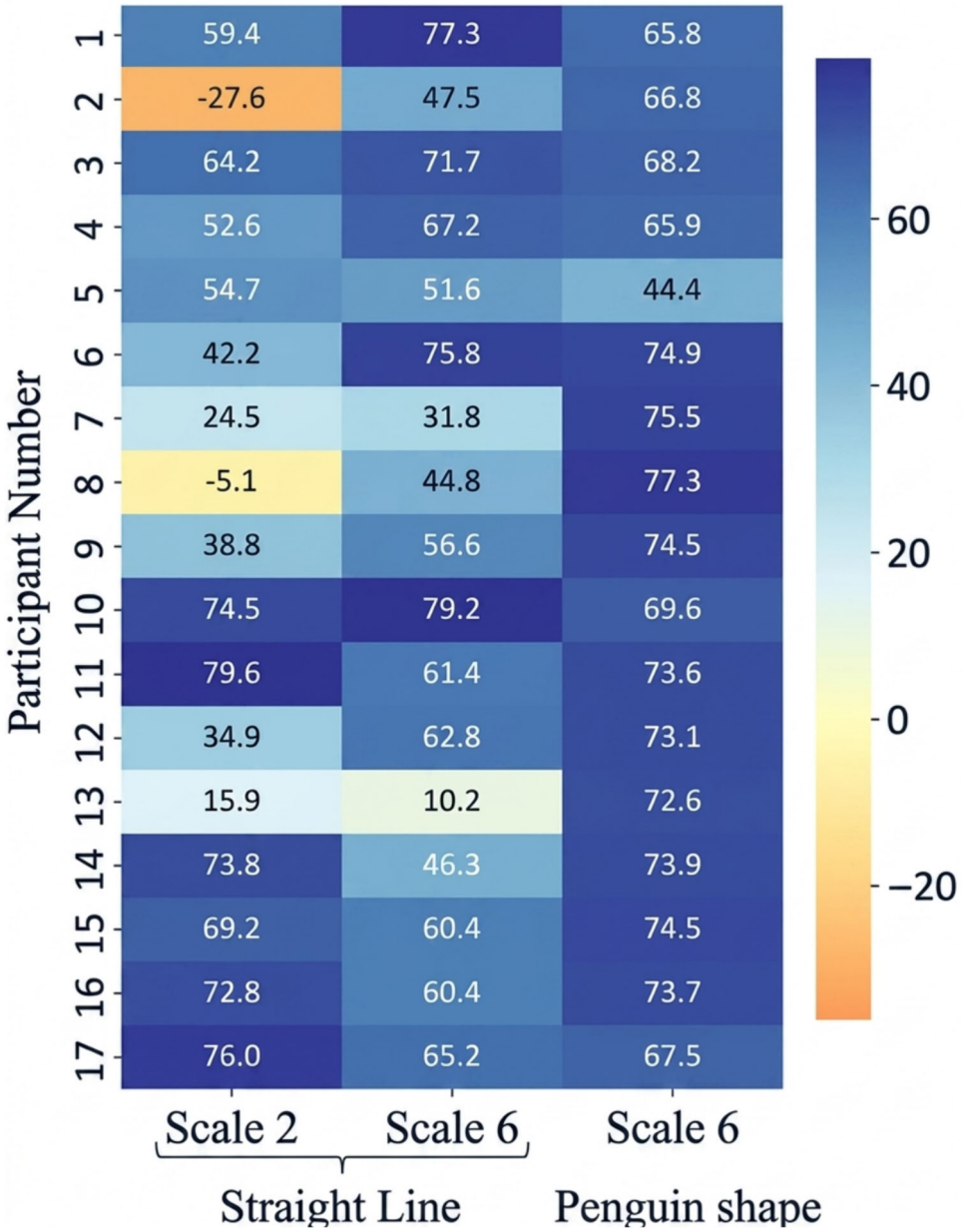


Fig. 11 Heatmap representing the distribution of performance scores across all participants

in achieving realistic conditions for remote grinding operations. The assessment of vibration-based haptic feedback (Fig. 12b) revealed that 17% of participants perceived the feedback as strong and realistic, and 65% considered it clear and helpful. Only one participant rated it as slightly noticeable. Several users reported mild hand fatigue or numbness after prolonged use, which may have reduced sensitivity to subtle vibration changes. Other comments highlighted that visuo-haptic features, such as color-coded force feedback and particle effects, became more dominant and perceptually influential as the task progressed. Overall, the haptic system effectively conveyed tactile information, enhancing realism and control during teleoperation. Figure 12c summarizes the evaluation of the workspace-scaling feature. The majority of participants (76%) rated this function as very helpful, emphasizing its contribution to motion precision and overall ease of operation. The results confirm that adjustable scaling improves fine manipulation, particularly in detailed or delicate tasks, and plays a significant role in facilitating human–robot skill transfer. The complete questionnaire materials are available in Supplementary Section S5, Figure S5-S12.

Table 3 Overall mean correlation values for Scale 6 across user experiment tests

Task type	Mean of correlation coefficient (%)	Max	Min	Standard deviation
Straight line	0.86	0.98	0.76	0.061
Penguin shape	0.94	0.98	0.92	0.018

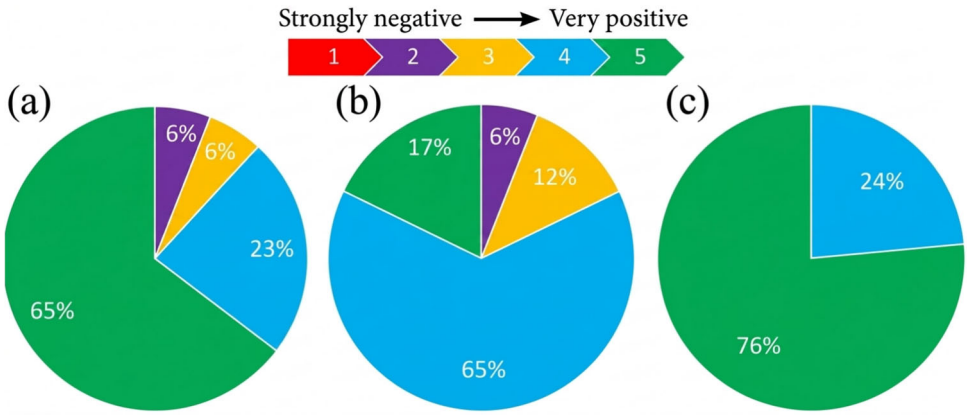


Fig. 12 Results of the user experience post-Questionnaire test; (**a**) immersion in the Unity application, (**b**) perceived intensity of haptic feedback, and (c) usefulness of surface scaling in Unity for control precision

3.5 Current limitations and future research directions

The experimental evaluation presented in this work focuses on validating the teleoperation interface and the system's ability to capture and reproduce human demonstrations. The tasks used in the experiments are simplified surface interaction scenarios designed to evaluate motion reproduction, interaction forces, and user experience. The study therefore primarily investigates the human–robot interaction interface and the demonstration-based programming workflow rather than the optimization of low-level robot control. In the presented implementation, robot motion is executed through velocity commands transmitted via ROS 2, while the underlying joint-level control and servo regulation are handled by the built-in controller of the UR10e industrial robot. The control strategy therefore serves as enabling infrastructure for the teleoperation platform rather than a contribution of this work. The study also does not aim to provide a full manufacturing process validation of grinding or polishing in terms of metrics such as material removal rate, surface roughness, or tool wear. Instead, the experiments evaluate platform-level performance characteristics, including system responsiveness, trajectory reproducibility, force interaction awareness, and user usability within representative surface interaction tasks. Furthermore, the present work does not include comparative benchmarking against alternative robot teaching approaches such as kinesthetic teaching, visual-only teleoperation, or conventional industrial programming methods. The primary objective of this study is the development and validation of a visuo–haptic teleoperation platform integrating virtual reality interaction, vibrotactile feedback, and demonstration-based programming within a unified framework. At present, widely established benchmarking protocols for such integrated visuo–haptic teleoperation systems remain limited. Future work will extend the platform toward manufacturing-specific experiments and investigate learning-based approaches for generalizing demonstrated tasks to new geometries and process conditions. In addition, future research may explore the development of benchmarking methodologies for immersive visuo–haptic teleoperation systems, enabling more systematic evaluation of such interaction frameworks.

4 Conclusion

This study presented a visuo–haptic virtual-reality teleoperation platform designed to support demonstration-based programming of force-sensitive robotic tasks through intuitive human–robot interaction. The proposed system integrates a ROS2-based control architecture with real-time velocity tracking, visuo-haptic feedback, and autonomous playback functionalities. The robot operates under Cartesian velocity commands transmitted through ROS 2, while the underlying joint-level control and servo regulation are handled by the built-in controller of the UR10e industrial robot. Force awareness is conveyed through both visual and haptic modalities. Vibration intensity is proportional to the measured contact force, while a color-coded interface displays real-time numerical and graphical indicators of the applied force. Within the virtual environment, users interacted with a scalable grinding surface that could be enlarged up to tenfold, enhancing ergonomics and motion precision. Experimental

validation confirmed an end-to-end latency below 15 ms and positional accuracy within 5 mm, demonstrating the system's responsiveness and reliability. Force regulation tests showed that contact forces remained within the safe operational range of 17–22 N. Trajectory correlation coefficients exceeding 0.8 indicated strong repeatability and reliable reproduction of demonstrated trajectories between operator demonstrations and robotic playback. Minor systematic errors were identified, likely due to network bandwidth constraints that affected data transmission during trajectory playback. The user study highlighted the system's intuitiveness and immersive design. Participants reported high satisfaction with the VR environment and described the haptic feedback as clear and realistic. Furthermore, the creation of a virtual twin with workspace scaling was found to enhance motion precision and task performance while reducing the effects of tracker latency. Visuo-haptic cues were also perceived as more dominant and informative than vibration-only feedback. Overall, these findings confirm that the proposed platform provides an intuitive, responsive, and reliable solution for demonstration capture and autonomous trajectory replay in force-sensitive robotic manipulation tasks. Future work should focus on developing open, Linux-compatible tracker drivers to enable transparent calibration and improve tracking accuracy. Replacing existing MoveIt dependencies with custom ROS2-based modules could further enhance system robustness and interoperability. Additionally, integrating advanced closed-loop force sensing and adaptive control strategies could extend the platform toward more demanding manufacturing processes such as robotic grinding and polishing.

Supplementary Information The online version contains supplementary material available at https://doi.org/10.1007/s12008-026-02600-x.

Funding This research was funded under the Program 'Innovative Hochschule'(Innovative University) by the Federal Ministry of Research, Technology and Space (BMFTR) of Germany (Grant No. 13IHS232C) and the City of Hamburg. The article processing charges were supported by the Open Access Publishing Funding Program of Hamburg University of Technology.

Declarations

Conflict of interest The authors declare that they have no conflict of interest.

Open Access This article is licensed under a Creative Commons Attribution 4.0 International License, which permits use, sharing, adaptation, distribution and reproduction in any medium or format, as long as you give appropriate credit to the original author(s) and the source, provide a link to the Creative Commons licence, and indicate if changes were made. The images or other third party material in this article are included in the article's Creative Commons licence, unless indicated otherwise in a credit line to the material. If material is not included in the article's Creative Commons licence and your intended use is not permitted by statutory regulation or exceeds the permitted use, you will need to obtain permission directly from the copyright holder. To view a copy of this licence, visit http://creativecommons.org/licenses/by/4.0/.

References

1. Long, Y., et al.: A review of contact-based robotic micromanipulation systems: technology and applications. J. Intell. Robot. Syst. **111**(3), 89 (2025)
2. Deng, Y., et al.: A novel positioning accuracy improvement method for polishing robot based on Levenberg–Marquardt and Opposition-based Learning Squirrel Search Algorithm. J. Intell. Robot. Syst. **110**(1), 8 (2023)
3. Verna, E., et al.: Real-time monitoring of human and process performance parameters in collaborative assembly systems using multivariate control charts. J. Intell. Robot. Syst. **110**(3), 126 (2024)
4. Ke, X., et al.: Review on robot-assisted polishing: status and future trends. Robot. Comput. Integr. Manuf. **80**, 102482 (2023)
5. Bilancia, P., et al.: An overview of industrial robots control and programming approaches. Appl. Sci. (2023). https://doi.org/10.3390/app13042582
6. Ham, H., et al.: Teleoperation of soft robots with real-time fingertip haptic feedback using small batteries. Adv. Mater. Technol. **8**(15), 2300070 (2023)
7. Li, W., et al.: Learning from demonstration for autonomous generation of robotic trajectory: status quo and forward-looking overview. Adv. Eng. Inform. **62**, 102625 (2024)
8. Kaiser, J., et al.: Learning to reproduce visually similar movements by minimizing event-based prediction error. In: 2018 7th IEEE International Conference on Biomedical Robotics and Biomechatronics (Biorob) (2018)
9. Galarza, B.R., et al.: Virtual reality teleoperation system for mobile robot manipulation. Robotics (2023). https://doi.org/10.3390/robotics12060163
10. Kim, Y., Sloth, C., Kramberger, A.: Skill transfer for surface finishing tasks based on estimation of key parameters. In :2022 IEEE 18th International Conference on Automation Science and Engineering (CASE) (2022)
11. Ochoa, H., Cortesão, R.: Control architecture for robotic-assisted polishing tasks based on human skills. In: IECON 2019 - 45th Annual Conference of the IEEE Industrial Electronics Society (2019)
12. Ochoa, H., Cortesão, R.: Impedance control architecture for robotic-assisted mold polishing based on human demonstration. IEEE Trans. Ind. Electron. **69**(4), 3822–3830 (2022)
13. Zeng, X., et al.: Surface polishing by industrial robots: a review. Int. J. Adv. Manuf. Technol. **125**(9), 3981–4012 (2023)
14. Nemec, B., et al.:Learning by demonstration and adaptation of finishing operations using virtual mechanism approach. In: 2018 IEEE International Conference on Robotics and Automation (ICRA) (2018)
15. Borrell, J., et al.: Cooperative human–robot polishing for the task of patina growing on high-quality leather shoes. Int. J. Adv. Manuf. Technol. **125**(5), 2467–2484 (2023)
16. Hoebert, T., et al.: A framework for enhanced human–robot collaboration during disassembly using digital twin and virtual reality. Robotics (2024). https://doi.org/10.3390/robotics13070104
17. Müller, F., Koch, M., Hasse, A.: User study to validate the performance of an offline robot programming method that enables robot-independent kinesthetic instruction through the use of augmented reality and motion capturing. Robotics (2024). https://doi.org/10.3390/robotics13030035

18. González, C., et al.: Advanced teleoperation and control system for industrial robots based on augmented virtuality and haptic feedback. J. Manuf. Syst. **59**, 283–298 (2021)
19. Cheng, R., et al.: On muscle activation for improving robotic rehabilitation after spinal cord injury. In: 2018 IEEE/RSJ International Conference on Intelligent Robots and Systems (IROS) (2018)
20. Sun, C., et al.: Fully autonomous real-world reinforcement learning with applications to mobile manipulation, In: Proceedings of the 5th Conference on Robot Learning, F. Aleksandra, H. David, and N. Gerhard, Editors.(2022), PMLR: Proceedings of Machine Learning Research. p. 308—319
21. Whitney, D., et al.: Comparing robot grasping teleoperation across desktop and virtual reality with ROS reality. In Robotics Research. (2020). Cham: Springer International Publishing
22. Judakova, Z., et al.: Sensitivity of cell cultures on time-varying low-frequency magnetic field changes. Appl. Sci. (2023). https://doi.org/10.3390/app13031777
23. Elnwegy, A., Youssef, F., Kern, T.A.: Study to compare different transmission procedures in the context of a robotic telemanipulation system. Measurement: Sensors **38**, 101847 (2025)
24. Song, D. K., Goldberg, N.Y., Chong, Networked telerobots, in *Springer Handbook of Robotics*, B. Siciliano and O. Khatib, Editors. 2008, Springer Berlin Heidelberg: Berlin, Heidelberg. p. 759–771

Publisher's Note Springer Nature remains neutral with regard to jurisdictional claims in published maps and institutional affiliations.

Authors and Affiliations

Mohammad Sadeghi[1,2] · Julio Cesar Ceron Espejo[1] · Thorsten A. Kern[1,2]

✉ Thorsten A. Kern
t.a.kern@tuhh.de

[1] Institute for Mechatronics in Mechanics, Hamburg University of Technology (TUHH), Eissendorferstr 38, 21073 Hamburg, Germany

[2] Haptic Lab, Ligeti Center - Laboratories for Innovation and General-Audience Edification Through the Transfer of Ideas, Veritaskai 1, 21079 Hamburg, Germany